

# POINT-SPRING MODELING OF THE GRASP OF A DEFORMABLE OBJECT BY AN ANGULAR GRIPPER

Nicolas Mouazé<sup>1</sup>, Lionel Birglen<sup>1</sup>

<sup>1</sup>*Robotics Laboratory, Department of Mechanical Engineering, Polytechnique Montréal, Montréal, QC, Canada*  
*Corresponding author: Nicolas Mouazé (e-mail: nicolas.mouaze@polymtl.ca)*

---

## ABSTRACT

The accurate evaluation of the deformation undergone by a soft object when it is seized by a gripper has many important applications but remains a difficult challenge due to the computational burden associated with this task. For instance, during surgery excessive pressure has been associated with local trauma (microlesions) leading to undesirable bleeding. For produce pick and place, the same type of excessive pressure can cause unsightly bruises and unnecessary waste as these damaged produces generally cannot be sold to the customer. In this paper, an alternative to the usual Finite-Element Analysis (FEA) method is used to accelerate the computation of an effective model, simpler but keeping excellent accuracy. While introduced in a previous work by the authors, this model is here refined by analyzing the impact on the simulation accuracy of the number of elements used to approximate the soft object. The latter being critical for computation efficiency. Simulations are discussed here with the objective of confirming what is the minimal viable number of elements one can use in the case of an angular gripper grasping deformable circles of various radii. After the introduction of the numerical model, comparisons with FEA of the results obtained from the model depending on the number of elements are shown. Finally, experiments with a surgical forceps and deformable cylinders confirm the effectiveness of the model in producing accurate results.

**Keywords:** Mass-spring model; grasping interaction; deformation modeling.

---

## MODÈLE POINT-RESSORT POUR LA SAISIE D'UN OBJET DÉFORMABLE PAR UNE PINCE ANGULAIRE

### RÉSUMÉ

L'évaluation précise de la déformation subie par un objet mou lorsqu'il est saisi par un préhenseur a de nombreuses applications importantes mais reste un défi difficile à relever en raison de la charge de calcul associée à cette tâche. Par exemple, lors d'une opération chirurgicale, une pression locale excessive peut être associée à un traumatisme local (micro-lésions) entraînant des saignements indésirables. Pour la manipulation de produits agricoles, ce même type de pression excessive peut causer des traces disgracieuses menant à des pertes inutiles, car ces produits endommagés ne peuvent habituellement pas être vendus au client. Dans ce document, une alternative à la méthode habituelle d'analyse par éléments finis est utilisée pour accélérer le calcul d'un modèle efficace tout en conservant une excellente précision. Bien qu'introduit dans un travail précédent par les auteurs, ce modèle est ici affiné en analysant l'impact sur la précision de la simulation du nombre d'éléments utilisés pour approcher la forme de l'objet mou. Ce nombre étant essentiel pour l'efficacité du calcul. Des simulations sont discutées dans le but de confirmer quel est le nombre minimal viable d'éléments que l'on peut utiliser dans le cas d'une pince angulaire saisissant des cercles déformables avec différents rayons. Après l'introduction du modèle numérique, des comparaisons avec l'analyse par éléments finis des résultats obtenus à partir du modèle en fonction du nombre d'éléments sont présentées. Enfin, des expériences avec une pince chirurgicale et des cylindres déformables confirment l'efficacité du modèle à produire des résultats précis.

**Mots-clés :** Modèle masse-ressort ; saisie ; modélisation de déformation.

## 1. INTRODUCTION

Design optimization of grippers intended for the grasp or interaction with deformable objects usually involves the comparison and therefore, simulations, of a significant number of architectures. These simulations are typically relying on a Finite Element Method (FEM) which is the most widely software approach used for structural analysis. This method is accurate, but also requires significant computation time [1, 2] which makes certain optimization techniques difficult to use such as genetic algorithms, especially when large deformations are required. Another method referred to as mass-spring model (MSM) is commonly used for real-time application because of its simplicity and speed [3]. It consists of using mass points to discretize the geometries of the deformable objects to be simulated. These mass points are connected by springs approximating the elasticity of the material. In the available literature, values for the spring stiffnesses in a MSM are estimated with different techniques usually taking into account the geometry of the discretization (area of contiguous polygons, lengths, etc.) and material properties (Young's modulus, Poisson's ratio) [4–6]. Although stiffness evaluation processes are usually for two-dimensions cases, an adaptation for three-dimensional scenarios including masses localized at the discretized points has also been recently proposed [7].

The current most common application of MSM is visual effect for animation, where the goal is to quickly visualize realistic motions but not necessary accurate ones [8]. This trade-off is not acceptable for all applications especially when it can have important practical consequences, such as with surgery simulators where inaccurate results can have negative impact on training [9]. However, MSM can be made significantly more accurate, even for large deformation, when enough points are considered. In [10] a point-spring model (PSM), a MSM with no mass, was used to evaluate the deformation of a soft object grasped by compliant grippers with multiple architectures. The possibility to quickly go from one design to another and obtaining quick results from the simulation was the rationale of the choice of method and the results were shown to comparable to FEA at a much lighter computational burden. In this method, the points of the PSM only discretize the object contour shape and its fixed center, keeping complexity at a minimum. When forces are applied on the contour points, the internal springs of the model deform to mimic the flexibility of the soft material constituting the object. Thereby, deformations undergone by the object can be evaluated to optimize gripper design architectures. An example of application of this type of simulation is when one needs to design a medical tool minimizing the deformation, or at least mitigate damage, of fragile tissues or organs while keeping a maximum number of contact points for a secure grasp [11, 12].

One challenge of the aforementioned optimization is to determine the parameters of a PSM discretization for the soft object which will be both accurate and quick. As FEM, a simulation with a coarse meshing may not result in a reasonably accurate value while better results with a finer mesh are expected but may be very long to compute. The work presented in [13] focused on the validation of the numerical equations modeling grippers with deformable objects in order to fit with experimental measurements but without concerns about the required computational time. For instance, the number of divisions of the objects was not a parameter analyzed in the latter reference despite its critical importance for computation time and accuracy). In this article, different numbers of elastic elements are studied to evaluate a PSM simulating the grasp of a deformable circle by an angular (rotational) gripper. First, the numerical model of the object, the jaws of the gripper, and their interaction will be detailed. Then, a comparison of the accuracy of a discretization depending on its number of elements will be presented to determine the best distribution of contour points of the PSM for efficiency (accuracy and speed). Finally, PSM simulations are compared to experiments with a commercial surgical forceps and soft cylinders.

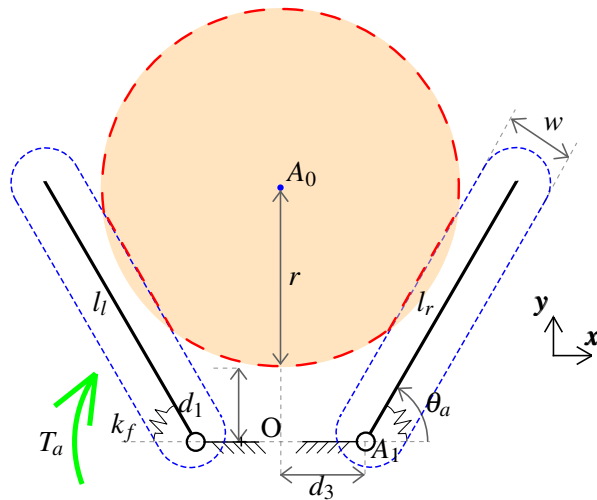


Fig. 1. Model of the gripper with a deformable soft object in red dotted line.

## 2. MODEL

Figure 1 illustrates the grasping scenario discussed in this paper: an angular gripper is squeezing a round soft object. The fingers of the gripper are symmetrical and the center of the object is assumed to lie along that axis of symmetry. For legibility purpose, the parameters in Fig. 1 are shown only for one finger. When an actuation torque  $T_a$  is applied on both fingers simultaneously (assumed identical and shown as a green arrow in the figure), the gripper closes to squeeze the object. The object shown at rest in orange then deforms along the dotted red line due to the contact pressure from the fingers. The angle  $\theta_a$  is the actuation angle and its value at rest is  $\theta_{a_0}$  in the following sections. A torsion spring with stiffness  $k_f$  is attached to both revolute joints to statically constrain the gripper when  $T_a > 0$  but before it makes contact with object. Thus, when the actuation torques vanish the fingers go back to their initial positions with this model.

Figure 2 presents a potential discretization of the object with a PSM. Points and springs define triangles and it should be noted that all points except the center belong to the contour of the object. The center point is used in this paper to fix the center of the object to the ground. As mentioned in the introduction, this discretization was selected for its simplicity. Appropriate spring stiffnesses are calculated depending on the Young's modulus and Poisson's ratio of the simulated material and contiguous triangles geometry as proposed in [14]. For example, the stiffness estimate of the spring between the green and blue triangle in Fig. 2 depends not only on the material but on the areas of these triangles and their lengths ( $r$  and  $h$ ). The contour points are assumed to be uniformly distributed along the circle. Their number are defined as the number of triangles and all contour springs have the same stiffness coefficients (noted  $k_{ext}$ ) as well as the internal spring (noted  $k_{int}$ ). When decomposing a round object in that manner, care must be taken to avoid a discretization leading to triangles with internal angles over  $90^\circ$  as it leads to negative stiffness with the Van Gelder model [14].

The numerical model proposed in [13] and laying the foundation of the present paper requires three steps as well as a few hypotheses that need to be recalled here. First, the motions are assumed slow and gravity is negligible compared to the grasp forces. Then, frictionless contact forces are modelled and thus, these contact forces are perpendicular to the finger surface. As for the methodology steps, the equation of the generated contact forces  $\mathbf{f}_p$  on the phalanges of an underactuated finger on rigid objects introduced in [15] is first used. This equation relates these contact forces to an input torque vector  $\mathbf{t}$  and also introduces matrices depending on the transmission mechanism (the Transmission matrix  $\mathbf{T}$ ), the geometry of the finger

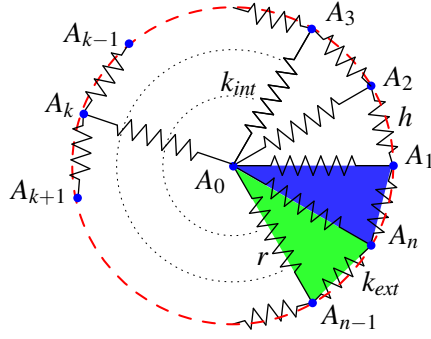


Fig. 2. Point-Spring Model of a Circular Object.

as well as the contact locations (the Jacobian matrix  $\mathbf{J}$ ), i.e.:

$$\mathbf{f}_p^T \mathbf{J} = \mathbf{t}^T \mathbf{T}, \quad (1)$$

with :

$$\mathbf{f}_p = [f_1 \quad \dots \quad f_p]^T \quad (2)$$

$$\mathbf{t}_{\text{gripper}} = \begin{bmatrix} T_a \\ -k_f \Delta \theta_a \\ -k_2 \Delta \theta_2 \\ \vdots \\ -k_p \Delta \theta_p \end{bmatrix} \quad (3)$$

where  $\theta_i$  and  $k_i$  ( $i \in [2, p]$ ) are the interphalanx angles and spring stiffnesses at the joints between them. The Transmission matrix corresponding to the angular gripper is simply:

$$\mathbf{T}_{\text{gripper}} = \begin{bmatrix} 1 & 0 & \dots & 0 \\ & \mathbf{I} & & \end{bmatrix} \quad (4)$$

and the grasp Jacobian matrix is:

$$\mathbf{J} = \begin{bmatrix} \mathbf{r}_{11}^T \mathbf{x}_1 & 0 & 0 & \dots & 0 \\ \mathbf{r}_{12}^T \mathbf{x}_2 & \mathbf{r}_{22}^T \mathbf{x}_2 & 0 & \dots & 0 \\ \dots & \dots & \dots & \dots & \dots \\ \mathbf{r}_{1p}^T \mathbf{x}_p & \mathbf{r}_{2p}^T \mathbf{x}_p & \mathbf{r}_{3p}^T \mathbf{x}_p & \dots & \mathbf{r}_{pp}^T \mathbf{x}_p \end{bmatrix} \quad (5)$$

where  $\mathbf{r}_{ki}$  is the vector from point  $A_k$  to the  $i^{\text{th}}$  contact point and  $\mathbf{x}_i$  the unit vector along the  $i^{\text{th}}$  phalanx in the direction of the end of the finger.

While Eq. (1) has been extensively used for underactuated hands, it can also be used for a fully-actuated gripper as considered here but needs to be adapted. Indeed, if the number of contact per phalanx is greater than one, the model of [15] is invalid and this situation is clearly to be expected for the interaction of the angular gripper with a PSM based soft object, especially when it starts to be squeezed. In [13], a methodology is presented to overcome this limitation of the original model. In order to use the equation for  $p > 0$  contacts on one finger, the latter is virtually divided into  $p$  links, or phalanges, connected by revolute joints. Each virtual joint is also combined with a stiff rotational spring ( $k_2$  to  $k_p$ ). Therefore, Eq. (1) becomes valid again since there is again only one contact per (virtual) phalanx and can be used to model the

interaction between the finger and the points of the PSM. In the modeled scenario of the rotational finger, the relationship between the input torques (due to the actuation and the springs) has to be calculated twice, one for each finger, since the finger positions are not expected to always be equal when the discretization is non-symmetrical.

The second step of the algorithm is the computation of the relationship between  $\mathbf{f}_o$  the vector of internal forces in the PSM and  $\mathbf{u}$  the vector of the displacements of all the object points as presented in [13]. This relationship can be expressed as:

$$\mathbf{f}_o = \mathbf{S}\mathbf{u} - \mathbf{P}\mathbf{k} \quad (6)$$

where  $\mathbf{f}_o$  and  $\mathbf{u}$  are vectors defined as:

$$\mathbf{f}_o = [f_x^1 \ f_y^1 \ \dots \ f_x^i \ f_y^i \ \dots \ f_x^n \ f_y^n]^T \quad (7)$$

$$\mathbf{u} = [\mathbf{u}_1^T \ \dots \ \mathbf{u}_i^T \ \dots \ \mathbf{u}_n^T]^T \quad (8)$$

with  $\mathbf{u}_i$  the displacement vectors of points  $A_i$  (see Fig. 2). The scalars  $f_x^i$  and  $f_y^i$  are the components of the forces at the endpoints of the  $i^{th}$  spring projected along the  $x$  and  $y$  axes of the reference frame (using subscripts  $x$  or  $y$  to indicate which axis). The matrices  $\mathbf{S}$ ,  $\mathbf{P}$  and vector  $\mathbf{k}$  depend on the stiffnesses and the positions of the points. Details on how to compute these matrices can be found in [13].

Finally, the last step is to establish a connection between Eq. (1) and (6). This can be done by using the the projection matrices defined in [13] and the resulting equations are:

$$\mathbf{f}_p = \mathbf{D}_x \mathbf{f}_o, \quad (9)$$

$$\mathbf{f}_p = \mathbf{D}_y \mathbf{f}_o, \quad (10)$$

$$\mathbf{0} = \mathbf{D}_z \mathbf{f}_o. \quad (11)$$

Matrices  $\mathbf{D}_x$  and  $\mathbf{D}_y$  associate each internal force applied on a point to the corresponding phalanx force. The forces are also projected to match the direction of the fixed frame. For phalanges not touching the PSM, their contact forces are equal to zero. Matrix  $\mathbf{D}_z$  completes the static equilibrium equations for the contour points not in contact with the phalanges.

From the initial position of the gripper and object pair, by increasing the input torques incrementally and solving Eqs. (9), (10) and (11) the motion of the finger and deformations of the PSM can be simulated efficiently. In the numerical examples of this paper, the model is implemented in Matlab and the difference between the left- and the righthand side of these equations are numerically minimized with a Nelder-Mead simplex algorithm.

### 3. NUMBER OF TRIANGLES

In this section, the accuracy of simulations with a PSM having different number of triangles are evaluated by simulating the grasp of a small ( $r = 5cm$ ), a medium ( $r = 7cm$ ) and a large ( $r = 10cm$ ) circle while varying the number of contour points. The simulated configurations are presented in Fig. 3 and the associated parameters are listed in Tab. 1 and 2. These results are obtained following the methodology of the previous section.

Starting from the approximation calculated with the Van Gelder model as an initial estimate, the spring stiffness values are calibrated to fit the results of a single corresponding FEA where a complete circle is grasped. A large number of elements is first used in the simulation, i.e. when a greater number does not affect the results significantly. Figure 4 illustrates an example comparing the angle  $\theta$  between the fingers for a specific input torque as calculated with an FEA software (ANSYS) and a PSM dividing the circle in 4, 12 and 20 triangles. Figure 5 shows for the three different sizes of circles the differences of position of the

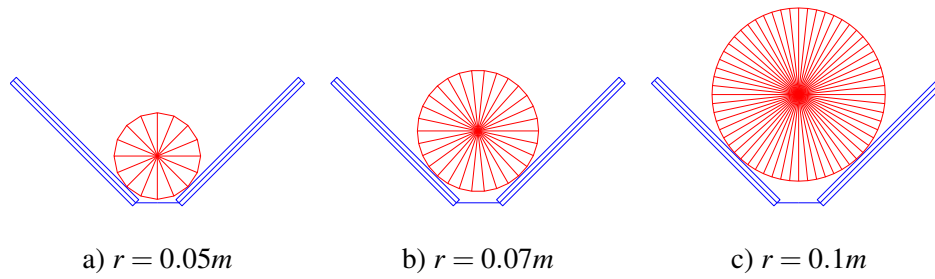


Fig. 3. Models of circular object grasped by a jaw gripper.

Table 1. Parameters of the finger in the simulation presented in Figs. 3, 4 and 5 (all lengths are in meters, angles in degrees, stiffnesses in  $N \cdot m$ ).

$l_r$	$l_l$	$\theta_{a_0}$	$d_3$	$w$	$k^f$
0.2	0.2	45	0.025	0.01	0.073

finger after deformations with four to sixty triangles. The required computation time with the medium size object is also illustrated in Fig. 6. For comparison, the FEA needs around 20,000s to compute one scenario.

From Fig. 4 and 5, one can observe that as expected the accuracy with a coarse mesh of the PSM is poor especially with the largest object. With a significant increase in the number of triangles, the results converge to a consistent difference. This was to be expected considering the same phenomenon appears with FEA. However, it is noticeable that accurate results can be obtained with a rather limited number of elements, especially again comparing with the FEA software. There is, however, a minimal number of elements to retain: a PSM with four divisions for example, namely a square, is clearly too far from the original geometry of the circle. During an optimization of a gripper with such a coarse discretization several architectures may be poorly evaluated. Obviously, the finer the discretization is, the closer the results fit with the FEA. With twelve points the evolution of the angle seems to converge to good results with most deformations. The object side in contact with the gripper is typically flattened and thus, positions of points aligned on the surface may not be as important as the number of those not in contact.

One can notice that the differences observed in Fig. 5 at sixty divisions (or more) are not zero. This is due to an imperfect calibration of the spring stiffnesses but this remaining error is small. Depending on the size of the object, the number of triangles to reach a prescribed range of accuracy varies. Indeed, the convergence depending on this number of elements is slower with a small object ( $r = 5cm$ ) but speeds up with larger radii. In this example, with twenty triangles or more, all results seem to match the FEA quite well, as the remaining gap with the FEA is not significantly improved if a finer discretization is tried. However, calculation time also increases exponentially (see Fig. 6) with more points to compute and therefore, this value (20) may be a good trade-off between computation time and accuracy. An identical evolution of calculation times was observed with the other objects. It should be noted that when the meshing is too fine, the use of virtual phalanx leads to convergence issue for the numerical model. Short distances between contour points imply short virtual phalanges in case of multiple contacts and thus, the relative angles between these phalanges become difficult to calculate.

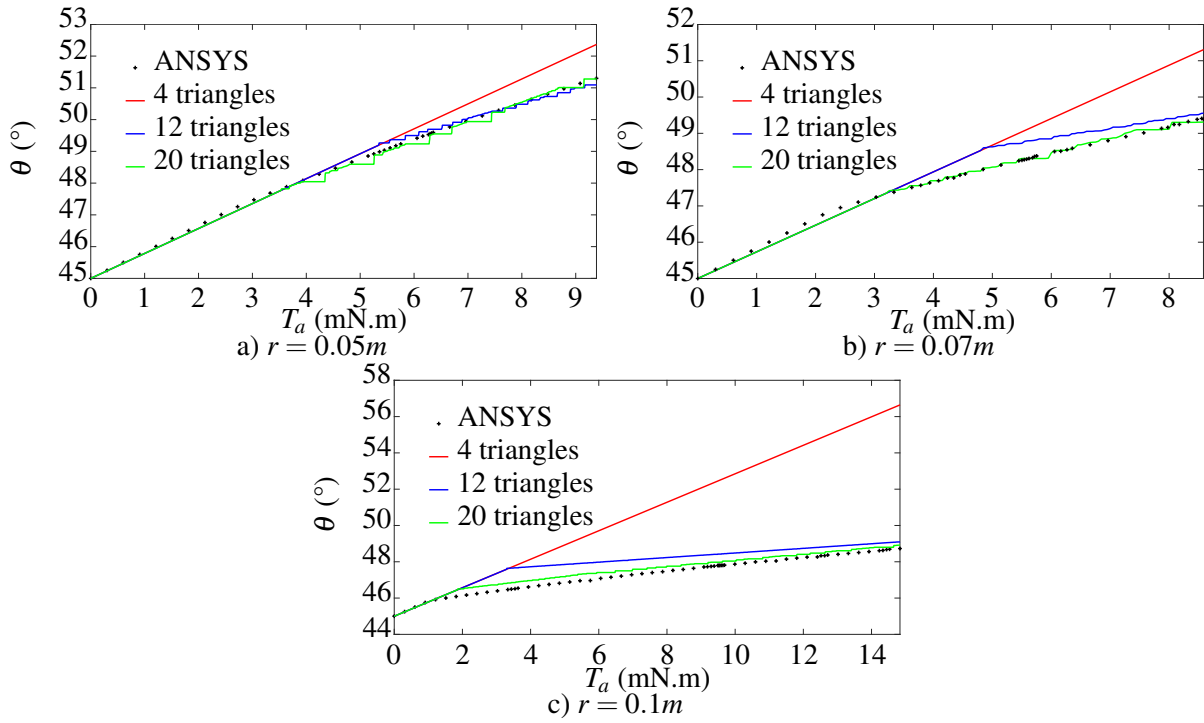


Fig. 4. Simulations with the numerical model compared to results with a FEA.

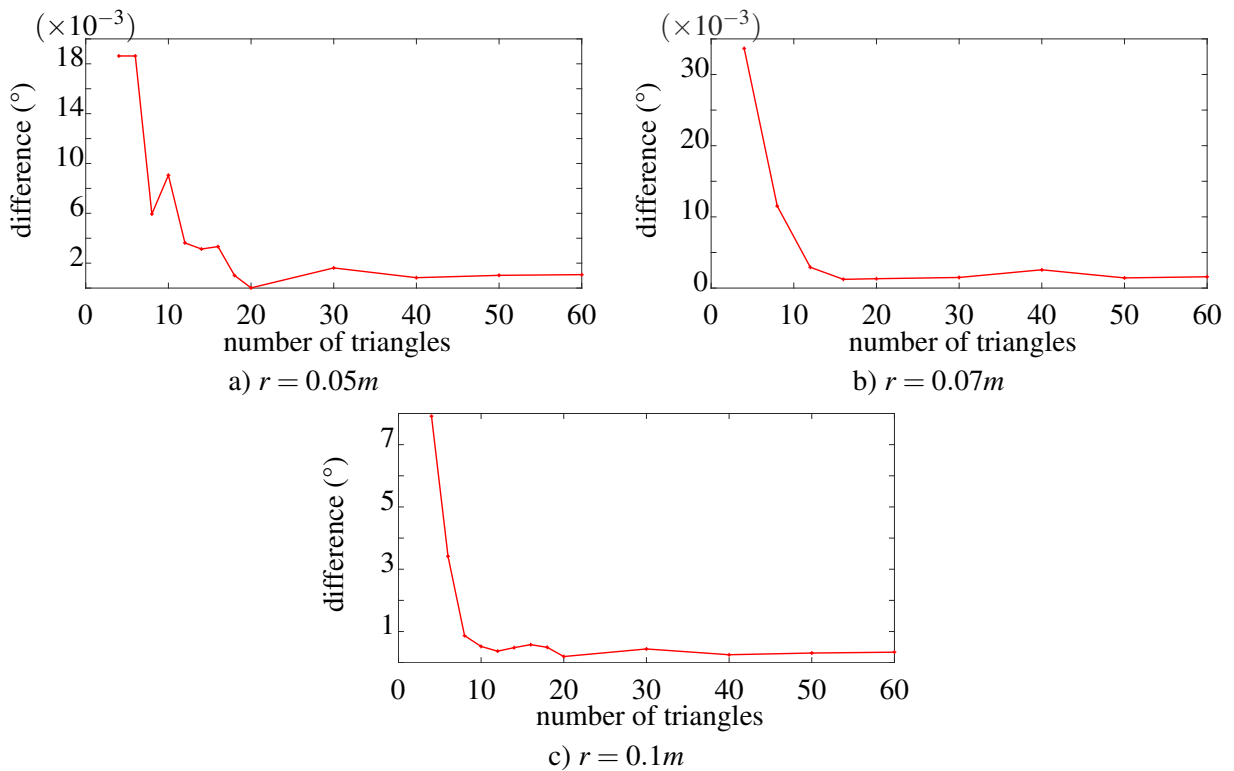


Fig. 5. Precision of the simulation depending on the number of triangles and circles with three different radii.

Table 2. Parameters of the object in the simulation presented in Fig. 3, 4 and 5 (all lengths are in meters)

$r$	$d_1$
0.05	0.004
0.07	0.013
0.1	0.025

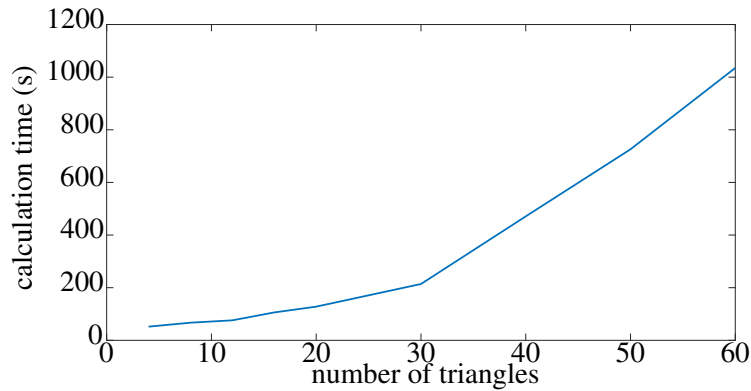


Fig. 6. Calculation times for different divisions of the object ( $r = 0.07$ ).

#### 4. EXPERIMENTS

To compare the proposed numerical model with experimental results, a surgical Hartmann alligator forceps (illustrated in Fig. 7) is used to grasp deformable circles. This forceps is driven close by the action of extension springs at the handle to provide a stable and consistent actuation torque at its jaws as a function of their openings. Figure 8 shows the forceps grasping many different soft circles. These circular objects were 3D printed with 100% infill using a thermoplastic polyurethane (PolyFlex TPU95). The finger spring of the model is in our case zero and the input torque  $T_a$  is created by the extension of the springs at the handle. To measure the actuation torque at the jaw of the forceps, a force sensor (Marveldex Force Sensing Resistor) was inserted during the grasp of several steel dowel pins with different diameters (instead of the soft object) to measure the generated forces, and in all experiments the angles between the jaws and the distance of contact were measured on pictures. The actuation torque  $T_a$  was then estimated for different openings of the forceps based on a linear interpolation. Figure 10 presents the torque from the measurements with the forceps and from the numerical model. After a calibration of the PSM to match the applied torque in one scenario by comparison between the experiment and a simulation (see Fig. 8(f) and 9(f)), the other grasps are simulated. The results corresponding to Fig. 8 are presented in Fig. 9. Based on the Young Modulus of the thermoplastic polyurethane used ( $E = 29MPa$ ) and the approximation of the Van Gelder model, a coefficient of 0.033 was applied to the spring stiffnesses to fit the simulation.

Tabs. 3 and 4 present the parameters of the finger and the objects, respectively. For the simulations, the spring value of  $k_f$  and the initial angles of the jaw are chosen arbitrarily. A spring value equal to zero would have led to an infinite number of possible position of the jaw. The torques due to this spring are therefore subtracted from the actuation torque in order to calculate the real torque applied on the object. The resulting torques correspond to the results shown in Fig. 10. These torques resulting from the model corresponding to the angle observed in the experiment are similar to the measured ones. The gap between the values may



Fig. 7. Surgical forceps.

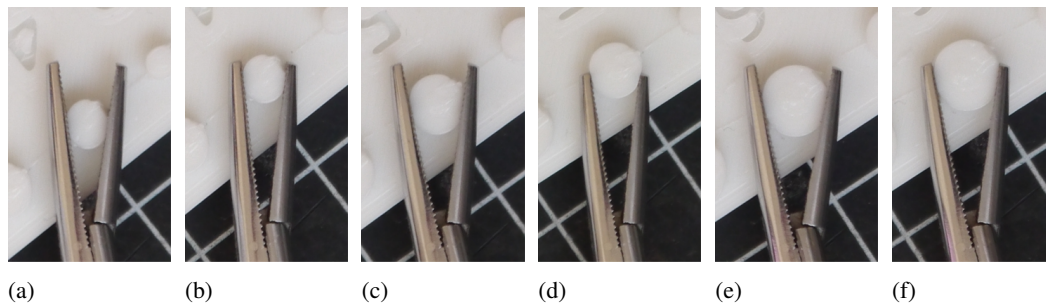


Fig. 8. Grasping by the forceps of circles with diameters of 4mm (a and b), 5mm (c and d) and 6mm (e and f).

be due to the lack of precision of the force sensor from which consistent readings were sometimes difficult to obtain.

Shapes of the deformed PSM also match the observed ones with the forceps. One example where both shapes from Figs. 8(d) and 9(d) are superposed is illustrated in Fig. 11. With the real and simulated jaws at the same position, the computed deformations are very close in all cases, event at the edge of the fingers where the curvature of the cylinder changed drastically. The small teeth on the forceps jaws also appear to have little influence of the deformation of the objects.

## 5. CONCLUSIONS

While a FEA produces accurate simulations, the calculation time and complexity of using this approach is a major drawback for certain applications, such as design optimizations or real-time rendering. Because of its simplicity, a PSM is shown here to be an alternative to achieve accurate simulations within a reasonable time. In this paper, a PSM was tested to simulate the interaction between an angular gripper and deformable circles. The goal was to find the trade-off between accuracy and calculation time in terms of number of elements used to approximate the circles with the ultimate objective to optimize future design of grippers. After a brief introduction of the model developed in a previous work, this model is used to evaluate the deformations of different sizes of objects depending on the number of triangles for different squeezing pressures and the calculation times are recorded. Twenty elements seem to be sufficient in most cases. However, to obtain the same level of accuracy, the results indicate that fewer elements are necessary with

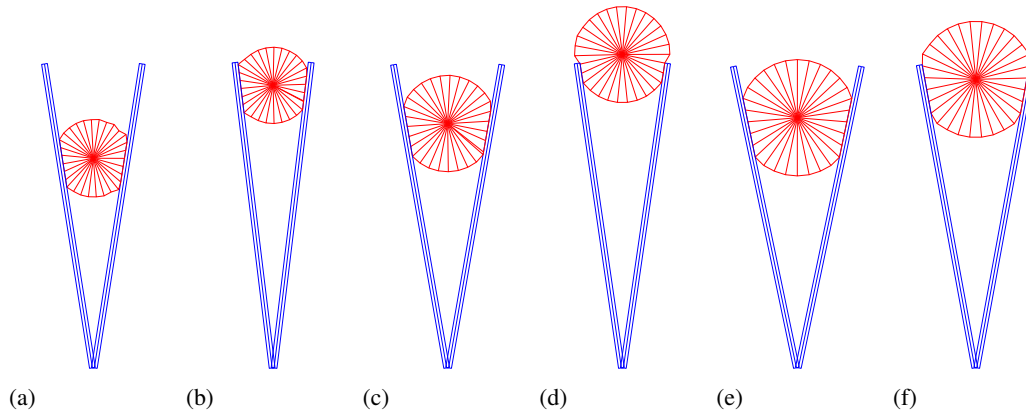


Fig. 9. Simulation of grasping by a forceps of cylinders with diameters of  $4\text{mm}$  (a and b),  $5\text{mm}$  (c and d) and  $6\text{mm}$  (e and f).

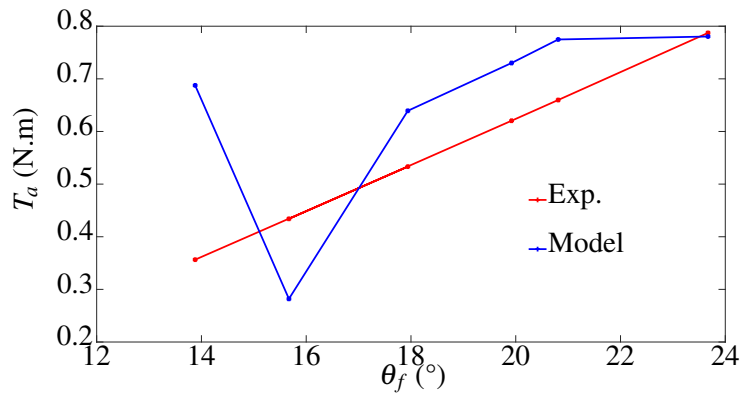


Fig. 10. Comparison between the torque from the model and experimental results.

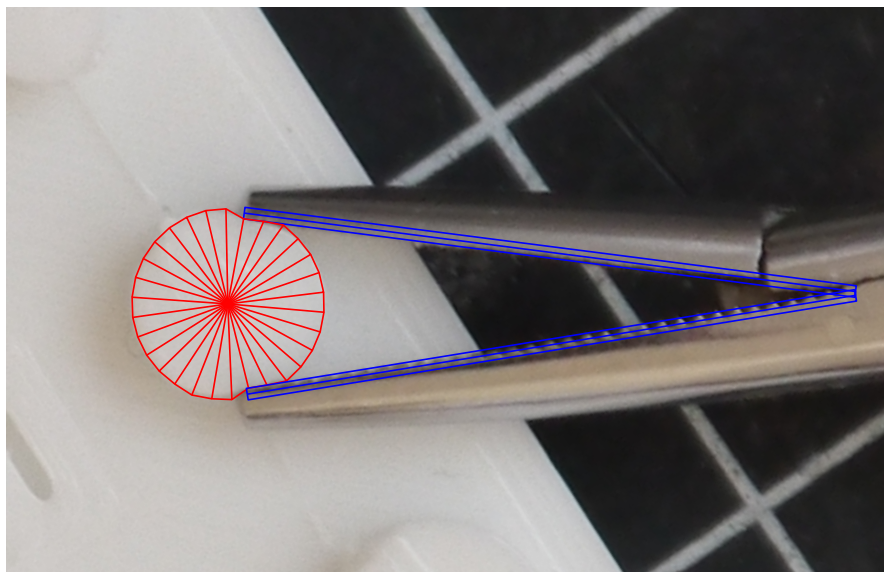


Fig. 11. Superposition of the deformed shape predicted by the model and an experimental picture ( $r = 2.5\text{mm}$ ,  $d_1 = 16\text{mm}$ ).

Table 3. Parameters of the finger in the simulation presented in Fig. 9 (all lengths are in millimeters)

$l_r$	$l_l$	$d_3$	$w$
16	16	0.1	0.3

Table 4. Parameters of the object in the simulations presented in Fig. 9 (all lengths are in millimeters).

	$r$	$d_1$
(a)	2	11
(b)	2	15
(c)	2.5	13
(d)	2.5	16
(e)	3	13
(f)	3	15

larger size objects (compared to the gripper). Finally, experimental observations with a surgical forceps grasping cylinders and the equivalent results from the numerical model are compared. This comparison yielded that both the experimental and simulated deformations are close to each other and thus, the model seems accurate.

## REFERENCES

1. Idkaidek, A. and Jasiuk, I. "Toward high-speed 3d nonlinear soft tissue deformation simulations using abaqus software." *Journal of robotic surgery*, Vol. 9, No. 4, pp. 299–310, 2015.
2. Sadraei, E., Moazzen, M.H., Moghaddam, M.M. and Sijani, F.S. "Real-time haptic simulation of soft tissue deformation." In "Robotics and Mechatronics (ICRoM), 2014 Second RSI/ISM International Conference on," pp. 053–058. IEEE, 2014.
3. Jiang, J., Sheng, B., Li, P., Ma, L., Tong, X. and Wu, E. "Real-time hair simulation with heptadiagonal decomposition on mass spring system." *Graphical Models*, p. 101077, 2020.
4. Baudet, V., Beuve, M., Jaillet, F., Shariat, B. and Zara, F. "Integrating Tensile Parameters in 3D Mass-Spring System." Working paper or preprint, February 2007.  
URL <https://hal.archives-ouvertes.fr/hal-01493738>
5. Bianchi, G., Harders, M. and Székely, G. "Mesh topology identification for mass-spring models." *Medical Image Computing and Computer-Assisted Intervention-MICCAI 2003*, pp. 50–58, 2003.
6. Zaidi, L., Bouzgarrou, B., Corrales, J., Mezouar, Y. and Sabourin, L. "Stable grasping of soft objects based on a 3d deformation model with visual and tactile feedback."
7. Golec, K., Paliernie, J.F., Zara, F., Nicolle, S. and Damiand, G. "Hybrid 3d mass-spring system for simulation of isotropic materials with any poisson's ratio." *The Visual Computer*, pp. 1–17, 2019.
8. De Oliveira, S.M., Vidal, C.A., Neto, J.B.C., De Carvalho, L.L. and Maia, J.G. "Cloth simulation with triangular mesh adaptivity." In "Graphics, Patterns and Images (SIBGRAPI), 2014 27th SIBGRAPI Conference on," pp. 235–242. IEEE, 2014.
9. Xu, L., Lu, Y. and Liu, Q. "Integrating viscoelastic mass spring dampers into position-based dynamics to simulate soft tissue deformation in real time." *Royal Society open science*, Vol. 5, No. 2, p. 171587, 2018.
10. Mouazé, N. and Birglen, L. "Deformation analysis of a compliant underactuated finger grasping a soft object."

- In “ASME 2018 International Design Engineering Technical Conferences and Computers and Information in Engineering Conference,” American Society of Mechanical Engineers Digital Collection, 2018.
11. Hong, M.B. and Jo, Y.H. “Design and evaluation of 2-dof compliant forceps with force-sensing capability for minimally invasive robot surgery.” *IEEE Transactions on Robotics*, Vol. 28, No. 4, pp. 932–941, 2012.
  12. Frecker, M.I., Powell, K.M. and Haluck, R. “Design of a multifunctional compliant instrument for minimally invasive surgery.” *Journal of biomechanical engineering*, Vol. 127, No. 6, pp. 990–993, 2005.
  13. Mouazé, N. and Birglen, L. “Deformation modeling of compliant robotic fingers grasping soft objects.” *Journal of Mechanisms and Robotics*, Vol. 13, No. 1, 2021.
  14. Gelder, A.V. “Approximate simulation of elastic membranes by triangulated spring meshes.” *Journal of graphics tools*, Vol. 3, No. 2, pp. 21–41, 1998.
  15. Birglen, L., Laliberté, T. and Gosselin, C.M. *Underactuated robotic hands*, Vol. 40. Springer, 2007.
  16. Baudet, V., Beuve, M., Jaillet, F., Shariat, B. and Zara, F. “Integrating tensile parameters in 3d mass-spring system.”, 2007.
  17. Nedel, L.P. and Thalmann, D. “Real time muscle deformations using mass-spring systems.” In “Proceedings. Computer Graphics International (Cat. No. 98EX149),” pp. 156–165. IEEE, 1998.